Chem Soc Rev

RSC Publishing

TUTORIAL REVIEW

View Article Online
View Journal | View Issue

Organic field-effect transistor sensors: a tutorial review

Luisa Torsi,* Maria Magliulo, Kyriaki Manoli and Gerardo Palazzo

Cite this: *Chem. Soc. Rev.*, 2013, **42**, 8612

Received 5th April 2013

DOI: 10.1039/c3cs60127g

www.rsc.org/csr

The functioning principles of electronic sensors based on organic semiconductor field-effect transistors (OFETs) are presented. The focus is on biological sensors but also chemical ones are reviewed to address general features. The field-induced electronic transport and the chemical and biological interactions for the sensing, each occurring at the relevant functional interface, are separately introduced. Once these key learning points have been acquired, the combined picture for the FET electronic sensing is proposed. The perspective use of such devices in point-of-care is introduced, after some basics on analytical biosensing systems are provided as well. This tutorial review includes also a necessary overview of the OFET sensing structures, but the focus will be on electronic rather than electrochemical detection. The differences among the structures are highlighted along with the implications on the performance level in terms of key analytical figures of merit such as: repeatability, sensitivity and selectivity.

Introduction

Electronic sensors are conceived to function as core elements in miniaturized, possibly fully integrated, systems capable of detecting a substance and delivering an already processed digital response. Such systems, also addressed as *smart sensors*, feature the integration of a microprocessor (embedded intelligence) along with the chosen sensor technology. Smart sensors are foreseen as capable of providing not just a customized output but also a significantly improved level of performance. The aim is to realize systems that are endowed with capabilities such as self-calibration, self-healing and the production of compensated measurements. The latter meaning the ability to produce an output signal that is already corrected for variables such as temperature, analyte concentration, interferents and base-line drift, to quote just the most relevant. All this would make smart systems performances desirably solid and reliable.

Dipartimento di Chimica Università degli Studi di Bari Aldo Moro & Consorzio Interuniversitario Sistemi a Grande Interfase – CSGI, Via Orabona 4, 70126 Bari, Italy. E-mail: luisa.torsi@uniba.it, maria.magliulo@uniba.it, kyriaki.manoli@uniba.it, gerardo.palazzo@uniba.it; Fax: +39 0805442092; Tel: +39 0805442092, +39 0805442019, +39 0805442018, +39 0805442028

Luisa Torsi

Luisa Torsi has been a full professor of Chemistry since 2005. She received her degree in Physics in 1989 and a PhD in Chemical Science in 1993. She was post-doctoral fellow at Bell Labs and has been awarded with the 2010 HE Merck prize, this marked the first time the award was given to a woman. Author of more than 100 ISI papers, including contributions published in Science, Nature Materials and Proceedings of the National Academy of Science. Her works gathered over 4400 citations resulting in an h-index of 32. Awarded research funding comprises several European contracts as well as national and regional projects.

Maria Magliulo

Maria Magliulo is researcher in Bio-Analytical Chemistry at the University of Bari. She graduated in Pharmaceutical Chemistry and Technologies at the University of Bologna in 2002 and received her PhD in Pharmaceutical Sciences in 2007 from the same University. In 2009 she joined the research group of Prof. Luisa Torsi in the Department of Chemistry, University of Bari. Her research focuses on the development of innovative, flow-assisted immunosensor formats and electronic biosensors based on Organic Field-Effect Transistors. She is author of more than 25 scientific publications in high impact factor journals and she has attended more than 70 international and national conferences.

Sensitive, selective, miniaturized, light-weight, low-power biosensing systems should be capable of providing information to the user wherever and whenever it is needed. In a more visionary scenario, the system is even expected to furnish the right information on what it is required to make sound decisions. A smart system for the detection of biological molecules of interest in clinical analyses (nucleic acids, metabolites, proteins, pathogens, human cells and drugs) would be ideal for application in what is addressed as point-of-care (POC) testing. Such a novel approach foresees clinical tests being performed at or near the site of patient care, namely at the medical doctor's office or even the patient's house, allowing for timely initiation of appropriate therapy and/or facilitating the linkages to care and referral. POC tests should in fact be simple enough to be used at the primary care level and in remote settings with no laboratory infrastructure. POC therefore has the potential to improve the management of diseases as well as of regular medical check-up testing.

This tutorial review aims at providing the necessary knowledge on the organic field-effect transistor (OFET) sensors,[1–4] highlighting the features that would make them ideal for POC applications. As the electrochemical OFET sensing configurations have been recently extensively reviewed[5,6] here the focus will be on electrolyte and back-gated OFETs biosensors.

In general OFET sensors use π-conjugated organic semiconductors (OSCs) as electronic materials and are endowed with biological recognition capabilities by proper functionalization or integration of bio-systems such as DNA strains, antibodies, enzymes and capturing proteins in general. The advantages over other sensing technologies such as electrochemical or optical based ones is the capability of delivering a response that is *label-free* using a simple electronic read-out set-up that can be easily miniaturized by also employing printed circuit technologies. Before going into the functional details of these devices it is worth mentioning that OFETs are developed in the framework of organic or plastic electronics technology[7] that is a relatively new field in which the device structures are based on organic materials being dielectric, conductive or semiconducting organic (macro)molecules. The revolutionary concept that is now turning into real prototypes, involves the realization of functioning electronic and opto-electronic devices (light-emitting diodes, photovoltaic cells, OFETs) and circuits by printing features on plastic or paper substrates using dielectric, conducting, insulating and semiconducting inks. Plastic electronic systems are produced at very low-cost using printing equipment instead of ultraclean high-tech fabrication facilities. The emerging field of organic electronics is therefore motivated by the possibility of mass-producing cheap and sustainable electronic devices and sensors. In Fig. 1 an example of inkjet printed, transparent OFETs on a flexible substrate, is featured.[8]

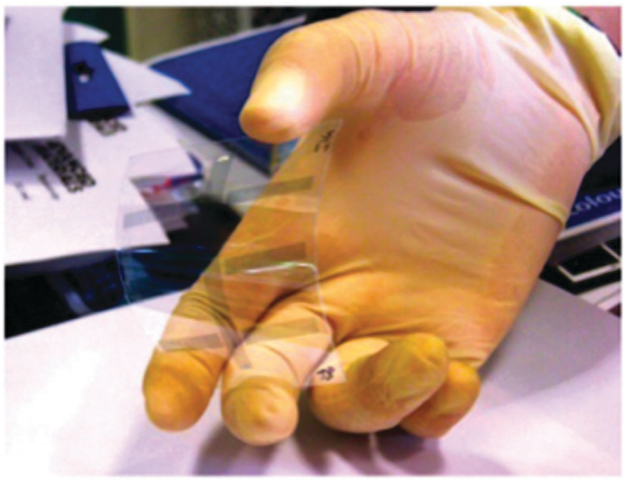

Fig. 1 Picture of transparent and flexible OFETs. Reprinted from ref. 8, copyright© 2011 Elsevier B.V., reproduced with permission from Elsevier.

Typical materials for OSCs include polymers such as poly(3-hexylthiophene) (P3HT) and alkyl-substituted triphenylamine polymers (PTAA) but also oligomers such as pentacene and its soluble derivatives as well as many other organic materials

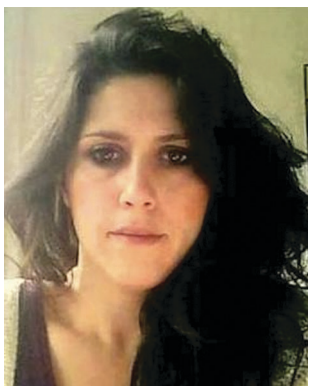

Kyriaki Manoli

Kyriaki Manoli received her BSc in Chemistry in 2003 from the University of Ioannina, Greece and her MSc and PhD in Polymer Science and its Applications from the Chemistry Department of the National and Kapodistrian University of Athens–Greece in 2005 and 2010 respectively. Both MSc and PhD thesis research were performed at the Institutes of Physical Chemistry and Microelectronics at National Center for Scientific Research "DEMOKRITOS" – Greece. Currently, she is working as a Postdoc at the University of Bari, Italy. Her research is focused on the fabrication and characterization of organic field effect transistors for sensing applications.

Gerardo Palazzo

Gerardo Palazzo is Associate Professor in Physical-Chemistry at the University of Bari. He received a degree in Chemistry in 1988 and a PhD in Applied Chemistry and Biochemistry in 2004. He has been the coordinator of several research projects of the Bari University and of CSGI. Currently he is the head of the degree courses (BS + MS) in Chemistry for Bari University. He has published more than 100 papers in international peer reviewed journals and books. His main research activities deal with the characterization of soft matter by means of physicochemical techniques, the biophysics of proteins and the development of novel biosensors.

capable of providing OFET devices with a mobility in excess of 1 cm^2 V s^{-1}.[9] More recently, natural and nature-inspired materials, such as indigoid dyes have been used as the active layer in OFETs that perform at the state-of-the-art level. Interestingly, these devices can be fabricated entirely from inexpensive and natural, biodegradable materials.[10] The driving force towards the use of OFETs as biosensors is the combination of the electronic output signal and the high sensing performance level with low-cost fabrication to develop disposable electronic sensing systems that would turn ideal for POC testing.

This tutorial review starts with an overview on what a biosensor is and the analytical figures of merit that need to be assessed are introduced in an operative manner. The importance of the *label-free* approach is highlighted too. This part is important as the analytical assessment is very seldom part of a study dealing with organic electronic sensors. OFETs are then introduced and their operation as chemical sensors is briefly presented. These are performing devices that, however, lack selectivity. To understand how to implement selectivity features, some OFET-relevant approaches to bio-functionalization are presented. The last section deals with the description of OFET biosensor configurations with particular attention to those involving electronic transduction. As anticipated, electrochemical OFET bio-sensors are not extensively discussed here.

An overview to biosensing and clinical testing

According to the International Union of Pure and Applied Chemistry (IUPAC) a biosensor is *a device that uses specific biochemical reactions mediated by isolated enzymes, immunosystems, tissues, organelles or whole cells to detect chemical compounds, usually by electrical, thermal or optical signals*. In other words, a biosensor is an analytical device involving biological recognition elements whose interaction with an analyte is turned into a measurable signal by a transducer. A block diagram of a biosensor is reported in Fig. 2.

Since the development of the first enzymatic biosensor by L. C. Clark and C. Lyons in the early sixties, there has been worldwide intense research activity on biosensors. Particularly, the success of glucometers, used to monitor the glucose blood concentration in diabetics, as well as the commercialization of lateral flow assays such as pregnancy tests, have led clinical diagnostics to be the most significant area for the application of biosensors particularly as POC systems. It is currently recognized that early diagnosis is an essential prerequisite for the prevention and treatment of diseases and can contribute to reducing the medical costs of healthcare services. The availability of sensitive, robust, affordable and rapid diagnostic tools, to be used outside of conventional clinical laboratories, can drastically contribute to reducing the number of deaths for infectious diseases such as HIV, tuberculosis and diarrheal infections in developing countries. It is worth mentioning that biosensors can be used to detect a wide range of clinically relevant targets present in biological fluids including blood, saliva, urine and even tears by just coupling the specific recognition elements to the transducer. For instance, enzymatic biosensors that use enzymes for the recognition process are mainly employed for the detection of metabolites such as glucose, lactate, urea, ammonia, creatinine, cholesterol and uric acid. These compounds are important diagnostic indicators of diseases such as diabetes, respiratory insufficiencies, kidney injury, hypertension, hyperthyroidism, ischemia and leukemia. On the other hand, biosensors based on affinity binding interactions (*i.e.* immuno-sensors such as the well-known pregnancy test) are principally used for screening proteins (including enzyme or antibodies), hormones and even whole cells that are biomarkers for cancer, cardiovascular, inflammatory and infectious diseases. Furthermore, geno-sensors, that employ nucleic acids as recognition elements, allow the detection of the presence of DNA or RNA in clinical samples in order to identify genomic or genetic-based pathologies. These biosensors are also widely employed to reveal the presence of infections caused by viruses, bacteria or fungi.

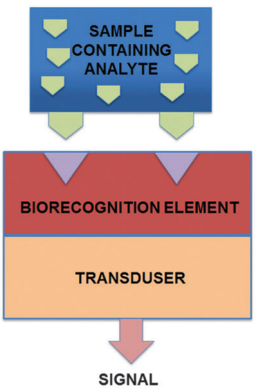

Fig. 2 Schematic representation of the main components of a biosensor.

Biosensing instruments designed for clinical applications can be divided into two types: high-throughput, sophisticated equipment mainly operated by skilled personnel for diagnostic or R&D purposes in clinical or research laboratories, and user-friendly, portable POC devices designed to be used directly by non-trained persons at the place where the monitoring is needed (*i.e.* doctor's office or patient's home). Implantable and wearable biosensors can be considered an alternative to the latter approach for monitoring physiological parameters such as blood oxygen levels or to continuously reveal analyte concentrations in biological fluids, in a non-invasive manner, in situations where personalized medicine is needed (diabetes, infertility, patients treated with anticoagulant drugs). OFET electronic sensors could be ideal for POC systems and the use of the recently introduced biodegradable or even sorbable systems would be interesting[10] for implantable devices.

As far as biosensors detection is concerned, two different signal transduction principles have been reported so far: *label-requiring* technologies in which the analyte or the recognition element are conjugated with an optical or electroactive probe that is revealed by the transducer, and *label-free* methods where a change in a physical variable, produced during the recognition

process, is directly measured. Electrochemical and optical label-requiring methods have been widely employed so far in the development of biosensors. As far as electrochemical detection is concerned, it mostly involves enzymatic amperometric biosensors.[11] In the simplest configuration, the glucose oxidase enzyme is immobilized underneath a semi-permeable membrane at the surface of a working electrode. The enzyme catalyses the reaction of glucose with oxygen, forming gluconolactone and hydrogen peroxide. The electrode membrane is permeable to the latter compound, which is oxidized at the working electrode. This oxidation produces a current that is proportional to the glucose concentration of the sample, allowing the monitoring of glucose concentration in blood. While electrochemical sensors can be easily adapted in portable and miniaturized devices at low cost, their full integration into a circuit (also as arrays) is not yet being reliably achieved. This is mostly connected to their need of a reference electrode whose integration into a circuit is still an open issue.[12]

Label-free technologies, thanks to their simple detection scheme (only one capture molecule is immobilized at the transducer detecting interface), are widely employed to monitor bio-affinity interactions and evaluate binding kinetic parameters in real time. Optical instruments based on Surface Plasmon Resonance (SPR) were the first to be proposed for biosensors development. For many years these devices have represented the gold standard in drug discovery and life science research. However, the complexity of the detecting apparatus as well as the high fabrication costs (adequate temperature control, accurate micro-fabrication processes and extraordinary quality optics needed) have driven researchers to investigate more simple and inexpensive techniques. Hence, technologies such as resonant mirror, diffraction gratings, interferometry, mechanical Quartz Crystal Microbalance, surface acoustic wave sensors, electrochemical impedance spectroscopy as well as electrical transduction devices such as ion sensitive FETs (*vide infra*), were developed. Although several of these *label-free* biosensors have shown good sensitivity, their integration in compact POC devices is still far from seeing the market horizon. An organic electronic biosensor, that does not need a reference electrode to be reliably operated, can represent a challenging opportunity for integration into a POC.

Analytical biosensors: the basics on performance figures of merit

Validation of an analytical method is an essential step to assess its capability to provide reliable qualitative or quantitative data. This applies also (and more compellingly) to a novel technology such as electronic biosensing. The analytical figures of merit that need to be assessed are selectivity, calibration range and linearity (along with sensitivity and limit of detection), precision, accuracy, limits of detection and quantification. Although several efforts have been made to internationally standardize the guidelines for bio-analytical method validations, there is still the need to clarify the meaning and interpretation of crucial aspects of sensing assay validation. These concepts are operatively introduced below.

Selectivity

In biosensors development it is very important to be sure that a given signal (response) is due only to the presence of the target analyte/analytes in an investigated sample. Selectivity is therefore the capability of the bio-analytical method to discriminate the analyte from interfering components such as other analytes or matrix components (metabolites, impurities, degradation products). According to IUPAC *the selectivity of a method refers to the extent to which it can determine particular analytes under given conditions in mixtures or matrices, simple or complex, without interferences from other components.* Specificity instead, is addressed as *the ultimate of selectivity*, *e.g.* 100% selectivity. The latter condition being by definition difficult to achieve, the term *selectivity* should be preferred to *specificity*. Among the different methods for biosensor selectivity determination, two are generally recommended. Operatively, the first one consists of measuring the biosensor response against interfering substance(s). In that, a calibration curve for each interfering substance is plotted and compared to the analyte calibration curve, every curve being measured under identical operating conditions. Selectivity is then expressed as the ratio of the signal output of the analyte (measured alone) to that of the interfering substance (measured alone) both at the same concentration. In the second procedure, interfering substances are added, at their expected concentration to a solution that already contains the analyte, dissolved at a concentration selected at the mid-range of the expected value. The selectivity is then expressed as the percentage of variation of the biosensor response. It is important to point out that, while a large number of bio-chemical (protein–protein, antibody–antigen, nucleic acid hybridization *etc.*) interactions can be ranked as *selective*, it is very seldom that chemical interactions, involving weak interaction forces, can be addressed as such. This is the reason why, to endow a sensor with selectivity capabilities, biological systems should be preferably implemented. As one of the few exceptions, quite selective detecting capability can be reached either by using organometallic complex chemistry to sense ions[13] or by exploiting catalytic interactions.[14] In any case a selective interaction should never be taken for granted but always duly demonstrated by one of the previously described procedures.

Calibration curve

The biosensor calibration is performed by evaluating the relationship existing, within a specified range, between the sensor response and the concentration of the analyte standard solutions. Five or more analyte standard solutions, covering at least two orders of magnitude of concentrations, are necessary for the calibration. When possible, physiological experimental conditions (in terms of analyte molarity, pH and ionic strength of the medium, *etc.*) should be used. The calibration standards should be evenly spaced over the concentration range of interest and they should be run at least in duplicate (preferably triplicate or more), and should be measured in a random order. The evaluation of responses from the negative control/blank (solution without analyte) is also required. The calibration curve is to be obtained by plotting the response (R) for the analyte standard

solutions (corrected for the background) *versus* the analyte concentrations or its logarithm. The use of normalized responses (*e.g.* $\Delta R/R_0$, where $\Delta R = R_{analyte} - R_0$ and R_0 is the blank response) is recommended. The linearity of the calibration curve is determined by an adequate regression analysis of the data.

The best operating conditions should be selected by comparing the results obtained with different calibration curves measured on the same or on different devices. In the former case the response *repeatability* and in the latter the *reproducibility* will be assessed. At each concentration level, the precision should be estimated by the relative standard deviation calculated as: RSD% = $(SD/R_{mean} \times 100)$ where SD is the standard deviation and R_{mean} is the biosensor's relative response averaged over at least three replicates as $\Delta R/R_0$. The pertinent regression parameters should be calculated for each experiment and, optionally, they can be statistically analyzed to determine intra- and inter-device variability.

LOD, LOQ and sensitivity

The Limit of Detection (LOD) is defined as *the lowest amount of an analyte in a sample which can be detected but not necessarily quantified as an exact value*. The LOD is expressed as a concentration corresponding to the smallest signal that can be detected with reasonable certainty for a given analytical procedure. The most common approach foresees the evaluation of a response to the analyte that is reliably above the signal coming from the blank solution (baseline). Operatively, the first step is to measure the responses of at least ten independently prepared blank samples, evaluating the corresponding mean (B_{mean}) and SD (σ_B) values. The LOD can be then calculated as the concentration corresponding to a response that is $B_{mean} \pm k\sigma_B$, whereby k is a numerical factor chosen according to the level of confidence required.[15] IUPAC recommends a value of $k = 3$ as the probability of a blank signal being 3-fold higher than the B_{mean} (*i.e.* a false positive) is less than 1%. The LOD may not be confused with the sensitivity of the method. The latter is *the capability to discriminate small differences in concentration or mass of the test analyte and is equal to the slope of the calibration curve*. The limit of quantification (LOQ) is defined as *the lowest concentration of an analyte in a sample that can be quantitatively determined with a given precision and accuracy*. Operatively, the LOQ is estimated by taking $k = 10$ in the LOD definition. The quantification range can be defined as *the range of concentration, including the higher and lower limit of quantifications, that can be reliably and reproducibly quantified with accuracy and precision through the use of a concentration–response relationship*. Finally, it has to be pointed out that the LOD and LOQ values, in the case of biosensors based on bio-recognition processes, directly correlate with the relevant dissociation constant. Indeed, the LOD is lower for analytes with lower dissociation constants and higher for analytes with higher dissociation constants (*i.e.* with lower binding affinities). Moreover, the biosensor response will be always negligible for concentrations much lower than the dissociation constant. In Fig. 3 a calibration curve along with the LOD and the LOQ are reported for a streptavidin OFET biosensor. The LOD is 10 nM while the LOQ is 18 nM while the streptavidin–biotin dissociation constant is in the fM range.

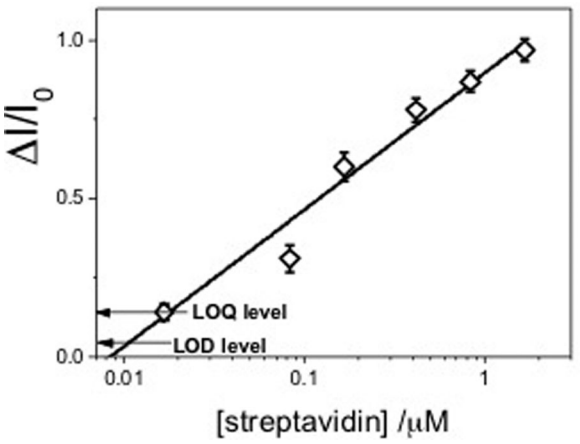

Fig. 3 A typical calibration curve showing the response as a fractional current increment of an electrolyte-gated OFET biosensor to streptavidin (*vide infra*). The LOD and the LOQ levels are graphically represented on the calibration curve.

Organic field-effect transistors

Before entering into the details of the OFETs sensors an introduction to the basic functioning principles of an organic field-effect transistor is necessary. First introduced in the 1980s,[16] OFETs have now reached performance levels comparable to that of their polycrystalline inorganic homologue and a number of p-type and n-type organic semiconducting materials with different chemical and physical properties exhibiting field-effect mobilities higher than 1 $cm^2\ V\ s^{-1}$ can be found.[9]

A typical OFET structure is shown in Fig. 4a, while Fig. 4b shows the device exposed to a gaseous atmosphere.

In its simplest form, an OFET comprises a gate contact that is defined on the substrate which could be rigid (a silicon wafer) or flexible (plastic or even paper). Resorbable materials[17] have also been recently introduced, demonstrating that the whole device can be dissolved in few days. Implantable POC applications with such a technology would allow the step of system removal after use to be avoided. The gate electrode is in

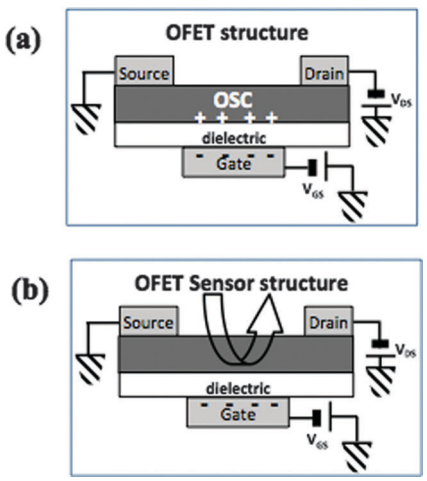

Fig. 4 Scheme of a typical OFET device structure before (a) and after exposure to an analyte (b).

contact with a dielectric that is interfaced to the OSC film. The gate dielectric should have a high capacitance either because it holds a high dielectric constant k, or because it is a thin-film as will be discussed later.

The OSC can be made of oligomers or polymers that are deposited as films (a few tens of nanometers thick at most) by solution casting, spin coating or sublimation. Other deposition methods are also used, including printing techniques.[8] Solution processed OSCs are generally polycrystalline films composed of contiguous grains with linear dimensions of a few hundred nanometers.[18] Source and drain contacts to the OSC can be easily defined either by thermal evaporation through a screen-mask or again by printing. Gold is the most convenient contact metal because its work function is the closest to that of most p-type organic materials. For p-type OSCs the device is operated by independently negatively biasing the drain (D) and the gate (G) contacts applying the V_{DS} and V_{GS} potentials with respect to the grounded source (S). This is called *common source configuration*. Eventually a channel of positive charges, whose geometrical length (L) is the distance between the source and the drain pads, is formed between these contacts. The channel width (W) is the geometrical width of the pad.

A definitive model for OFET transport mechanisms and operation is still to be produced, nonetheless several reviews can be found that describe the present understanding very well.[19] Here only the most relevant aspects will be summarized in a rather phenomenological fashion. The metallic source and drain contacts are electrically connected to an OSC (p-type in this case) and are meant to inject and collect positive charges (see Fig. 4). Like most thin-film transistors, OFETs also operate in the so-called *accumulation mode* (*vide infra*) and a highly resistive OSC resulting in a low I_{DS} current in the *off* state ($V_{GS} = 0$) is necessary. The I_{DS} current flowing in the *on-state* ($V_{GS} < 0$) must be, instead, as high as possible. The switching between the two transport regimes is achieved as the gate-contact and the OSC channel are capacitively coupled through the dielectric layer, allowing positive charges to be accumulated and confined in the OSC at its interface with the dielectric layer. In that, V_{GS} controls the accumulation of charges at this interface while, under an imposed bias V_{DS}, the I_{DS} current flows between the source and drain electrodes. In other words, the field generated by the negative V_{GS} bias applied across the dielectric layer leads to a band-bending in the OSC as depicted in Fig. 5.

In Fig. 5a the band structures of the metal gate, the insulator (gate dielectric) and the OCS are depicted when no gate bias is imposed. The few positive charges in the OSC are due to the presence of p-type dopants whose control, at the ultra-low trace level, is very difficult, particularly in not fully ordered materials. Fig. 5b shows what happens at the interface when a negative V_{GS} is imposed. This generates a potential well that allows positive charges to be confined and accumulated at the OSC–dielectric interface, forming a conductive channel (between source and drain contacts) running through an ideal path perpendicular to the drawing plane. Due to this confinement the field-induced transport is two-dimensional (2D),[20] that is to say independent of the OSC thickness, provided that a continuous OSC thin layer is deposited.[21] Conversely the transport occurring at $V_{GS} = 0$ is three-dimensional (3D) as it involves the charges present in the whole p-type OSC film. The presence of these charges (that must be orders of magnitude lower than those induced by the gate field) is due to doping processes connected with the presence of impurities or structural defects that are difficult to control at the trace level. The field generated by the V_{DS} bias allows the charges present in the OSC potential well (OFET channel) to migrate in a direction perpendicular to the Fig. 5 plane. Indeed, the larger the negative gate bias, the

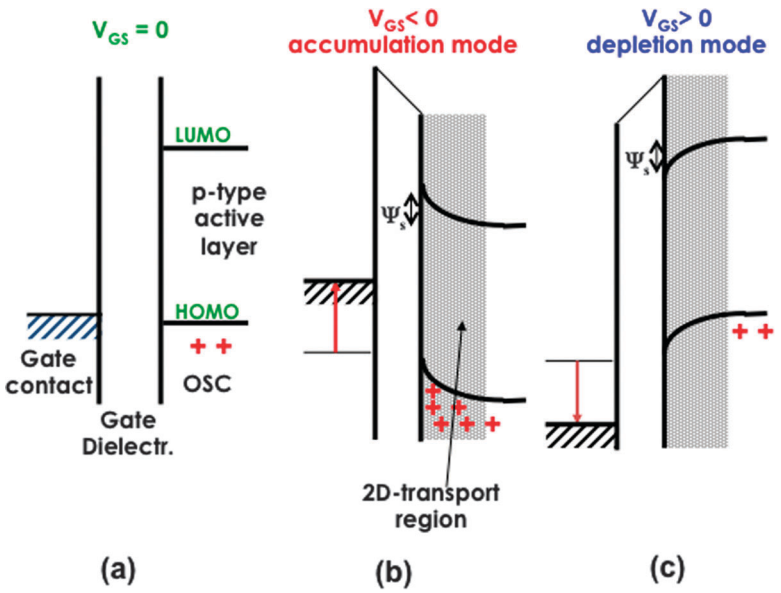

Fig. 5 Band diagram of metal–insulator–(p-type) semiconductor (MIS) structure at (a) zero gate ($V_{GS} = 0$), (b) accumulation ($V_{GS} < 0$) and (c) depletion ($V_{GS} > 0$) modes.

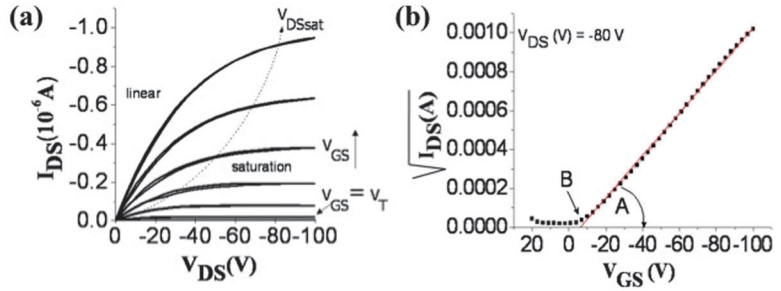

Fig. 6 (a) Current–voltage (I_{DS}–V_{DS}) characteristic curve of a P3HT p-channel OFET device at different V_{GS} gate voltages. The linear region at $V_{DS} < (V_{GS} - V_T)$ and saturation region at $V_{DS} > (V_{GS} - V_T)$, and $V_{DS}^{sat} = V_{GS} - V_T$ are evidenced. (b) Square root of the current–voltage (I_{DS}–V_{GS}) transfer characteristic measured at $V_{DS} = -80$ V. The linear regression is also evidenced.

larger the accumulated charge density, and the more intense the I_{DS} *on*-current is; this being the reason why this is addressed as *accumulation mode operation*. For an n-type OSC, negative charges are accumulated at the interface by applying positive V_{GS} bias and current flows for positive V_{DS}. To make sure that the transport in the channel is two-dimensional, it is necessary that the field generated by V_{GS} (normal to the channel plane) is always much larger than the one generated by the V_{DS} bias along the channel (*gradual channel approximation*). Again for a p-type OSC, if a positive gate voltage is applied, the field causes the semiconductor band edges (or more correctly the molecular HOMO and LUMO levels) to bend upwards, causing the positive charges to be accelerated towards the bulk of the OSC (Fig. 5c). The OFET channel region is then depleted and the I_{DS} current flow reduced (*depletion mode*).

The charge transport in the polycrystalline OSC involves carriers migrating through the channel region by hopping between the localized states present inside the band gap (energy gap between the HOMO and LUMO levels) of the OSC. These films are in fact systems comprising a narrow delocalized band associated with a high concentration of localized lower-energy electronic states that are located in the band gap and act as low mobility *trap* states.[22] The trapping states are also most probably originated by impurities and/or structural defects located in the crystalline grain or at grain boundaries.[23] Localized states in the OSC gap act as trapping or doping states depending on how stable a radical cation or anion is or equivalently how energetically close the localized state is to a delocalized molecular level. Indeed, traps are deep (far from the delocalized levels edges), low mobility states. The energy barrier between the grains is proportional to the surface density of charge traps at the grain boundaries themselves. In polycrystalline OSC materials transport takes place within a grain and across the boundary and, generally, the slower (rate determining step) process is the tunneling across the grain boundaries that causes the mobility to be limited by thermionic emission over the potential barrier at the grain boundaries.

As V_{GS} is applied the conditions for charge accumulation are set but the I_{DS} *on-current* flow does not start until a threshold gate voltage (V_T) is reached. This marks the gate bias needed to *turn the transistor on*. In thin-film transistors V_T is in fact equal to Q_{deep}/C_i where Q_{deep} is the density of charges that, once injected in the channel, are trapped, while C_i is the dielectric capacitance per unit area. So V_T is the gate voltage necessary to induce the charges required, Q_{deep}, to completely populate the deep trap energy levels. Once all traps are filled the further injected charges can migrate along the delocalized molecular orbital with a given mobility, through the channel under the imposed V_{DS} bias.

Typical current–voltage, *I*–*V*, curves for a P3HT p-channel OFET are shown in Fig. 6a.

As for all FET-based devices the set of I_{DS} currents is measured as a function of V_{DS} and each individual curve at a different, fixed V_{GS} bias. The curves are characterized by a *linear region* at $V_{DS} \ll (V_{GS} - V_T)$ and a *saturation region* at $V_{DS} > (V_{GS} - V_T)$. At low drain-source voltages the I_{DS} current follows Ohm's law being proportional to V_{DS} at a fixed V_{GS} (*linear regime*). In this regime the *gradual channel approximation* holds as the field generated by the gate potential is much larger the one generated by V_{DS}. As the drain-source voltage becomes more negative, a point is reached where the positive charges accumulated in the channel region are depleted at the drain contact region. As this ends the field along the channel (generated by V_{DS}) becomes too high compared to the gate one and the two-dimensional charge confinement is lost. The presence of this charge-depleted region generates a *pinch-off* of the channel and the current flow is limited to a constant value I_{DS}^{sat} (*saturation regime*). These features are well reproduced by the MOSFETs analytical expressions, generally used also to describe the OFET *I*–*V* curves. The equations are reported in the following:

$$I_{DS} = \frac{W}{L} C_i \mu (V_{GS} - V_T) V_{DS} \quad V_{DS} \ll (V_{GS} - V_T);\ \text{linear region} \tag{1}$$

Here W and L are the already introduced channel width and length, respectively; μ is the field-effect mobility ($cm^2\ V\ s^{-1}$), measuring how fast charges migrate under the imposed electric field. In the saturated region the following equation holds:

$$I_{DS}^{sat} = \frac{W}{2L} C_i \mu (V_{GS} - V_T)^2 \quad V_{DS} > (V_{GS} - V_T);\ \text{saturation regime} \tag{2}$$

Fig. 6b shows the square root of the I_{DS}^{sat} *vs.* V_{GS} transfer characteristic at constant V_{DS} taken in the saturation region.

The field-effect mobility, which is generally not constant in OFET devices, can be estimated from this curve. Operatively, eqn (2) can in fact be written as follows:

$$\sqrt{I_{DS}} = \sqrt{\frac{W}{2L}C_i\mu}V_{GS} - \sqrt{\frac{W}{2L}C_i\mu}V_T = AV_{GS} - B \qquad (3)$$

where the value of μ (from the saturated region) and V_T can be graphically extracted from the linear fit to eqn (3), reported as an example in Fig. 6b with A and B being the slope and the x-axis intercept:

$$\mu = \frac{2L}{WC_i}A^2 \qquad (4)$$

$$V_T = -\frac{B}{A} \qquad (5)$$

Typical values of μ for OFETs are in the 10^{-2}–10^{-1} $cm^2\ V\ s^{-1}$ range, but values as high as 1–10 $cm^2\ V\ s^{-1}$ can be easily measured.[9] Another figure of merit in an OFET is the *on*/*off* ratio, defined as the ratio between of the I_{DS} current values in the *on* and *off* states. This is indicative of switching performance of the device between the two distinct conduction regimes already introduced (2D and 3D) taking place in an OFET device.

As it is clear already from the basic description of the device electronic transport properties provided, OFETs are interfacial devices and the interplay between the dielectric and the OSC surfaces is complex and not yet completely understood. Nonetheless it is clearly received that the dielectric layer interfacial properties influence carrier transport and mobility in different ways. Specifically, the chemical and surface properties affect the morphology of the OSC and the orientation of small molecules or polymer segments. These impact on the transport properties that are strongly related to the molecules' orientation, as higher mobility hopping conduction is determined by the length of the π-delocalization. Moreover the semiconductor/dielectric interface roughness can modulate the mobility of charge carriers. This is the interface that will act as the key relevant one in the OFET sensing processes.

OFET chemical sensors

The use of an OFET for sensing purposes, in its simplest configuration, involves the direct exposure of the OSC to the atmosphere to be analyzed; in this case, the OSC acts both as the electronic transport material and as the sensing layer (Fig. 4b). The idea behind this approach is as simple as this: as an OFET is capable of generating a current amplification (indicated by the *on*/*off* ratio), wouldn't it be possible, once the OFET is exposed to an analyte, to also achieve a sensing response magnification? With this in mind the interaction of an analyte with an OFET was investigated by studying the changes induced in the transport properties upon exposure of the OSC to a target molecule. Operatively, the device I–V transfer characteristics (Fig. 6b) are measured in an inert atmosphere (N_2, pure water or buffer solution depending on the assay) and in the presence of the analyte; the changes of all the device parameters, (μ, V_T, I_{off} and the *on*/*off* ratio) are computed and correlated to the analyte concentration. Before entering into the details of the OFET sensor functioning it is important to anticipate that the OFET detection is *label-free* and it is also highly repeatable as demonstrated by several groups. It has been also demonstrated that it is sensitive and, upon proper functionalization with biological receptors, can be also selective.

OFETs were first proposed as chemical sensors in the late eighties[24] with one contribution[25] and one review published somehow later.[26] Some years after these few earlier reports, OFET sensors were proposed as multi-parametric sensors exploiting the possibility offered by an FET device of measuring, simultaneously and at room temperature, the variation of four electrical parameters. In this approach, pioneered in 2000,[27] the field-effect mobility and the *on*/*off* current ratio, as well as the threshold voltage and the bulk conductivity of the organic film, constitute the four output parameters used to characterize an OFET sensor's response to a given gaseous analyte. The bulk (3D) conductivity is typical of the OSC used as an active layer and could be measured in an equivalent resistor sensor, while the other parameters are characteristics of the 2D FET transport and can be easily extracted from the I–V transfer characteristics, as exemplified by eqn (4) and (5). Compared to the response of a homologue resistor the OFET provides three other parameters that can be used as an analyte finger-print. It is worth pointing out however, that the required selectivity, allowing us in principle to identify a species, is possible only if the OFET is endowed with recognition capability furnished typically only by a biological recognition element.

Besides the multi-parametric output, another advantage of the OFET response is the enhanced sensitivity. In Fig. 7a the analytical sensitivity (taken as the slope of the calibration curve) measured for an alkoxyphenilene-thiophene OFET exposed to a citronellol vapor, is plotted as a function of the device gate voltage.

As it is evident that the device sensitivity increases by three orders of magnitude when the applied gate voltage drives the OFET from the *off* to the *on* regime. In Fig. 7b the calibration curves for the same device (exposed to citronellol at fixed V_{GS} and V_{DS} bias) are reported for different OSC thicknesses. Although the film thickness is changed by one order of magnitude going from 95 nm to 950 nm, the device response is not significantly different at each measured concentration. This means that the OFET sensor response is indeed independent of the OSC thickness; that is to say it is 2D in nature, very much like the FET *on*-transport is. Both of these experiments[28] concur and demonstrate that there is a correlation between the amplified *on*-current flowing in the OFET channel and the enhanced sensing response evidencing how the FET amplified sensitivity can allow such types of electronic devices to outperform a resistor bearing the same OSC. Last but not least a further advantage of OFET sensors is that they are highly repeatable. When involving weak chemical interactions between the analyte and the OSC, the OFET response exhibits a repeatability with a standard deviation of up to a few percent over hundred subsequent exposures.[29–31] This relevant feature has been achieved

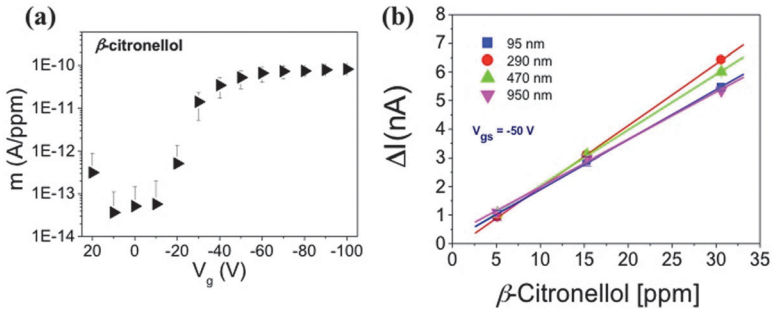

Fig. 7 (a) OFET sensitivity dependence on the gate voltage. Sensitivity values are determined from the slopes of the calibration curves (ΔI *vs.* analyte concentration) of an OFET device exposed to β-citronellol vapors at different gate biases, (b) current change (ΔI) at −50 V fixed V_{GS} and V_{DS} bias of OFET devices upon exposure to various concentrations of β-citronellol for different OSC film thicknesses. The data points are average values over three replicates.

by applying a pulsed reverse gate bias after a given exposure. As a matter of fact, if a trapping process occurs as a consequence of the interaction of the OSC with the analyte, the application of the positive gate bias (for a p-type OSC) reverses the band bending (Fig. 5c), and can allow the trapped charges to become free. It is in fact seen that by driving the OFET device in the depletion mode between two subsequent exposures allows the bias stress (transient current progressively setting to lower values) to be minimized and the response repeatability to be enhanced by restoring the original base line level before each new exposure.[29–31]

The sensing mechanism of OFET sensors that use the OSC also as an active layer upon exposure to a gaseous analyte (Fig. 4a) can be described by starting from the charge distribution at the semiconductor/dielectric interface region. Depending on the OSC properties and morphology, the analyte can cause changes in the threshold voltage and in mobility due to charge trapping/detrapping and increase/decrease of the potential barrier between continuous grains. As already anticipated, these effects result in a change of the drain source *on*-current and the 2D conductivity.[32] Moreover, OSCs are amenable to non-covalent π-interactions involving ionic bonds, hydrogen bonds and van der Waals forces. The analyte molecules can be adsorbed onto the surface of the grains, trapped in the free volume of the amorphous grain boundaries and even percolate through the voids between grains reaching the interface between the OSC with the gate dielectric or with the electrodes. Parameters such as the nature of the analyte (*e.g.* molecular size, dipole moment, electron affinity) and the size of the grain boundaries can affect the response of the sensor. To overcome issues such as sensitivity and cross-selectivity, modification of the semiconductor polymer's side chains with functional groups[33] or the addition of layers with molecular systems exhibiting some degree of affinity with the analyte, can lead to an increase of the binding affinity between the sensitive layer and the gas molecule. This strategy proved successful to reliably detect volatile organic compounds (VOCs) such as alcohols and ketones.[29] Gases such as NH_3 and NO_x involving transfer reactions also received considerable attention for their detection in environmental monitoring, the detection of explosives and disease diagnosis through breath analysis. Different active layers such as substituted thiophene-based polymers and oligomers, pentacene, metallophthalocyanines (MPCs) and metalloporphyrins (MPs) have been used in OFETs for nitro-based explosives,[34] ammonia,[35] nitric oxides[36,37] and peroxides[38] detection. Here the mechanism is such that the analyte induces a positive or a negative V_T shift, depending on the redox properties of the analyte. This can be explained by considering that V_T is sensitive to the charges injected into or withdrawn from the OSC. The electron-rich conjugated system, typical of OSCs, makes them sensitive to strong oxidants such as NO, hydrogen peroxide and nitroaromatic compounds, acting as electron acceptors that trap charges or dope the OSC layer. In this case the increase of I_{DS} and the positive shifts in V_T, have been observed in p-type materials. Different mechanisms have been proposed involving traps of negative charges due to analyte reduction at the OSC/dielectric interface[36] or accumulation of more holes due to oxidation of the semiconductor.[38] Opposite behaviour is seen when a p-type OSC-based OFET is exposed to a reducing agent such as NH_3. The analyte acts as an electron donor system, causing a decrease in the I_{DS} current and negative shifts in the threshold voltage. Generally, amines donate electrons from the sp^3-hybridized nitrogen atom to the conductive polymer cation.[39] The positive charge density is reduced in the OSC along with the on-current and V_T.[35]

Although most chemical sensors have the configuration of Fig. 4b, a few biosensors have also been proposed where the OSC acts both as an electronic and sensing layer. In this case the bio-recognition element is uniformly distributed in the whole bulk of the OSC.[40] This approach, although not the most efficient one as it involves a bio-interaction with the bulk while it is the interface that matters, has produced some interesting results in configurations that will be addressed later on in the text.

The discussion of inorganic FET chemical sensors is beyond the scope of this review, but it is relevant to recall a few important features, to understand gate-modulated OFET biosensors. FET sensors, first proposed more than forty years ago,[41] envisaged a silicon metal-oxide-semiconductor FET (MOSFET) device endowed with a sensing metallic or conducting polymer gate layer. The interaction in this configuration occurs between the analyte and the gate contact, eventually

leading to a modification of its electrochemical potential. This is mirrored by a V_T shift of the MOSFETs, as in this kind of FETs the threshold voltage is linearly correlated to the gate metal work function (or, equivalently, its electrochemical potential). Hydrogen detection, through the catalytic interaction with the palladium gate, was successfully achieved at very low concentrations. Also worth mentioning are the Ion Selective (IS) FET electrodes, detecting clinically relevant ionic species by means of a selective membrane gate coating.[42] These are chemical sensors based on the electrochemical interaction of the analyte with the gate layer. The main draw-back of ISFET-like sensors is the need for a reference electrode to control the potential that makes them less prone to use in array-type smart sensing systems.[12]

In general, the detection of concentrations as low as part-per-billions (but most commonly part-per-millions) can be achieved by using an OFET for gas and vapour sensors. Besides, the ability of OFET sensors to combine multi-parametric analysis and signal amplification has been also demonstrated. However, the real limitation of the OFET detection performed by using an OSC both as electronic and sensing layer is the very low degree of selectivity.

Bio-recognition events at functionalized OFET interfaces

To endow a sensor with selectivity capabilities it is necessary to implement molecules capable of strong interactions with a target analyte. Very often such systems are addressed as *receptors*. However, rigorously speaking a *receptor* is a *protein* located on the cell surface or inside the cell that, upon binding of a ligand (*e.g.* hormone or a neurotransmitter) induces a cellular response. Systems endowed, in a more general sense, with selectivity capabilities should be addressed as *recognition elements* or *capturing molecules*. They can have very different chemical natures, ranging from simple inorganic complexes to bio-macromolecules such as nucleic acids and proteins (indeed including also true *receptors*). A prerequisite for a system to be selective is for it to hold a very precise three-dimensional structure, particularly for the binding sites where molecular recognition takes place. Ideally, only the target molecule (ligand or analyte) should fit the stereochemistry of the recognition site. In addition, the molecular interactions involved should be strong enough to form a complex with the low dissociation constant required to achieve a low LOD and LOQ. The combination of stringent binding site stereochemistry and strong interactions can hardly be met by small molecules (ion recognition achieved through the formation of organometallic complexes[13] being a notable exception) and usually the recognition elements are based on a macromolecular structure in which a huge number of rather weak bonds (mainly H-bonds) furnish a large binding energy and a highly specific geometrical compatibility to the binding site. Since the elaborate organization of life requires specific molecular recognition, it is not surprising that most of the recognition elements currently used in biosensing are natural systems such as antibodies, enzymes, nucleic acids, receptors, or are molecules of natural origin (polypeptide and RNA-based aptamers). One of the legacies of this biological origin is their usually not high stability with respect to some harsh chemical and physical treatments. Exposure to organic solvents, extreme temperature, non-physiological pH or high salt concentrations along with adsorption to surfaces are all events that can potentially destroy the native conformation of macromolecules and limit their ability to selectively bind ligands. Therefore the steps used to anchor biological recognition elements onto the active surfaces of biosensors must be carefully chosen.

To endow an OFET sensor with selectivity capabilities, the recognition elements should be stably secured either through integration into the device structure or by chemically anchoring them on the OSC surface. In the latter case hydroxyl, carboxyl or amino groups need to be produced on the OSC surface to covalently link the recognition elements to it. One of the most popular reactions involves the activation of carboxylic acids by the *N*-ethyl-*N*′-(3-dimethylaminopropyl)-carbodiimide hydrochloride (EDC) and *N*-hydroxysuccinimide (NHS). *Route a* in Fig. 8A describes this approach recently proposed for DNA sensing.[43]

In this case, the OSC surface is coated by a –COOH-rich layer deposited by plasma enhanced chemical vapor deposition (PE-CVD) then the N-terminus of the peptide nucleic acid is conjugated to these carboxyls using EDC/NHS chemistry. The hybridization with complementary DNA strands leads to a measurable response. Such a strategy could be extended to proteins such as antibodies or enzymes but in such a case complications are foreseen in the presence of residues bearing a primary amine group (*e.g.* lysine). In such a case crosslinks with the OSC surface could take place not only at the N-terminus end of the polypeptide chain but also at the positions of lysine residues with an unpredictable impact on the protein functionality. In addition, the controlled attachment of different recognition elements is difficult to achieve, as well as the anchoring of membrane proteins.

Very recently, two strategies have been proposed that overcome these limitations by forming sensing platforms that permit the modular addition of different recognition elements. The first strategy exploits the physical chemistry of phospholipids (PLs), amphiphilic molecules that are the main components of biological membranes. PLs in water spontaneously self-assemble, forming bilayers that, under suitable conditions, close themselves forming spherical PL shells known as vesicles. PLs bearing many different chemical functionalities are commercially available so that vesicles of desired compositions can easily be prepared and, if required, membrane proteins can be embedded into their bilayers. This procedure[44] (*route b* in Fig. 8A) that starts again from the OSC coated with –COOH groups through PE-CVD and the EDC/NHS chemistry is here used to stably anchor vesicles containing NH_2-functionalized phospholipids. The vesicles also contain PLs bearing functional groups that can be used for subsequent coupling reactions or used directly as recognition elements (represented by blue triangles in the cartoon). Eventually, the anchored vesicles

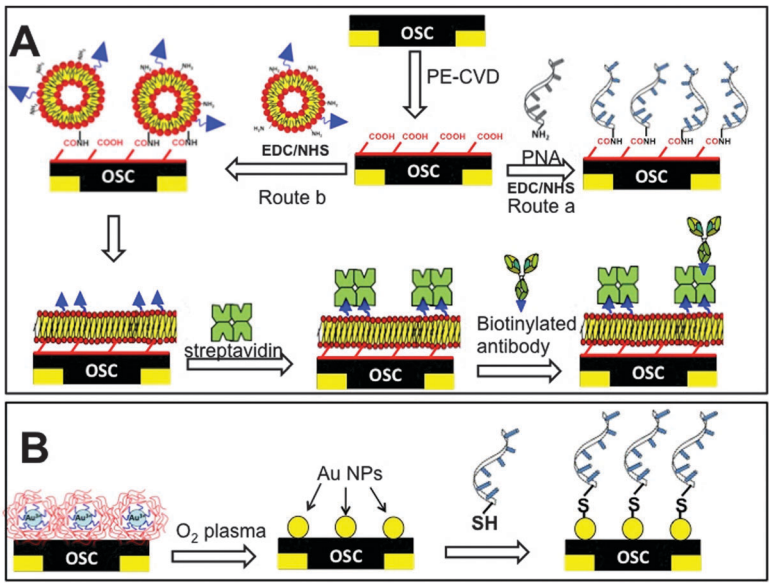

Fig. 8 (A) Plasma enhanced-chemical vapour deposition (PE-CVD) functionalization of the organic semiconductor surface with an hydrophilic coating characterized by carboxyl groups acting as anchor sites for biomolecules covalent attachment using the EDC/NHS chemistry. PNA strands (route a) for DNA detection, and biotynilated phospholipid layers (route b) for antibody well-oriented deposition, were anchored using this strategy. (B) Functionalization of the organic semiconductor surface with gold nanoparticles used for thiolated biomolecule immobilization.

spontaneously fuse, leading to the formation of a PL bilayer stably grafted at the OSC surface. Already this stage represents a surface that can be easily functionalized by exploiting the chemical groups linked to the PL. Numerous lipids are available for the attachment of proteins to the bilayer surface through amide, disulfide, thioether covalent conjugation or by means of biotin–streptavidin binding. In the original paper, PLs linked to biotin where used and the OFET was successfully able to sense streptavidin concentrations down to 10 nM. Moreover, the membrane-bound streptavidin still has biotin-binding sites available so that it is conceivable to use it to anchor biotinylated molecules such as antibodies.

An alternative approach is based on the thiol/gold chemistry. The procedure schematized in Fig. 8B is the following. A layer of micelles, formed by the poly(styrene-*b*-4-vinylpryidine) block-copolymer and containing $HAuCl_4$ in the pyridine core, is spun on the OSC surface. The micelles close-pack themselves at fixed center-to-center distances. Exposure to oxygen plasma leads to the total removal of the block-copolymer and the simultaneous reduction of auric ions to metallic gold, leading to an array of uniformly spaced gold nanoparticles on the OSC surface. This platform can then be easily functionalized by using thiol-bearing molecules, from thiolated DNA oligomers that bind Hg^{2+} or thrombin. The availability of thiolated chemicals allows for the incorporation of a broad range of molecules onto the surface of the sensor.[45]

Finally, very recently innovative OFET architectures have been proposed in which the biological recognition layer is integrated into the device by sandwiching it between the dielectric and the OSC (see next section for details). In such a case the biological recognition molecules are deposited on the dielectric surface (SiO_2) by simple spin coating or by the sequential electrostatic self-assembly of alternating layers of water-soluble positively and negatively charged polyelectrolytes (a procedure called layer-by-layer adsorption). Then the film of OSC is placed on top of the biological layer by spin-coating from organic solvent.

OFET biosensors

In the biosensor equivalent of an ISFET the bio-recognition elements, such as enzymes[46] but also antibodies/antigens, DNA and whole cells, are either deposited on the metallic gate (as depicted in Fig. 9a) or interfaced directly to the dielectric.

The analyte interacts with the recognition molecules layer giving rise to electrochemical reactions whose charged products can act as extra gating to the MOSFET, leading to a measurable V_T shift. Examples of this approach can be traced back to the earlier days of FET sensors and involve a MOSFET device.[41] More generally the interaction between the analyte and the recognition element can change the gate electrochemical potential. An example is reported in Fig. 9b where a standard MOSFET is a sensor that has a redox active gate contact – Ospolyvinylpyridine (Os-PVP) containing the enzyme horseradish peroxidase (HRP) – that exhibits a high sensitivity to H_2O_2.[46] The basic principle of the sensor is to measure the hydrogen peroxide concentration by measuring the change in the work function of the electro-active gate of the FET due to its redox reaction with H_2O_2. A constant current potentiometric mode is used to improve the sensitivity of the sensor. In such ISFET configurations however, no direct interfacing between the layer where the bio-chemical reaction takes place and the electronic channel is foreseen. Moreover, the detection is generally limited to electro-active or charged species. To overcome this limitation a labeling step is

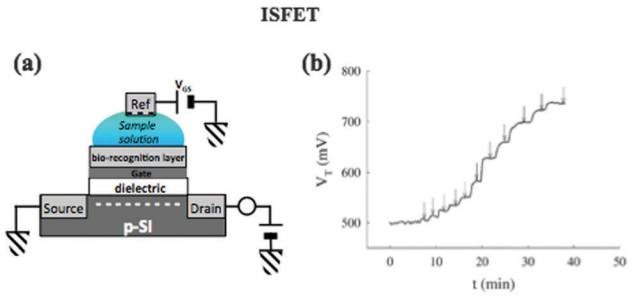

Fig. 9 (a) Scheme of an ISFET biosensor having the bio-recognition layer deposited on the metal contact surface. (b) Threshold voltage as a function of time for a MOSFET sensor with a redox active gate contact, including an horseradish peroxidase enzyme layer, as the peroxide concentration in water is changed. Reprinted from ref. 46, copyright© 2003 Elsevier Science B.V., reproduced with permission from Elsevier.

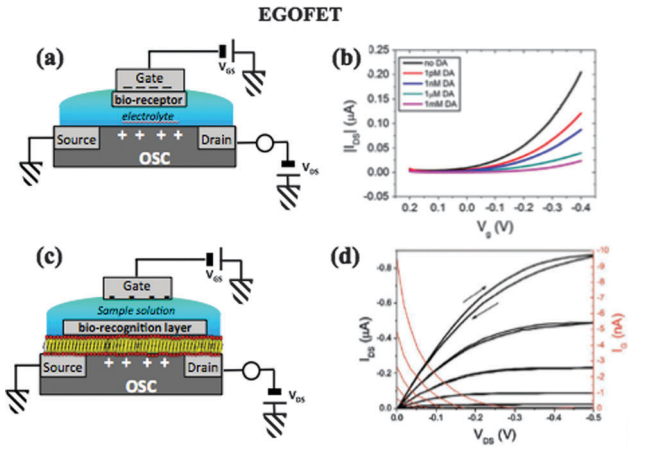

Fig. 10 (a) Typical structure of an EGOFET device. (b) I_{DS} *vs.* V_G transfer characteristic of a water-gated OFET where the gold gate is functionalized with a self-assembled monolayer of a boronic acid to sense different concentrations of dopamine. Reprinted from ref. 4, copyright© 2012 Elsevier B.V., reproduced with permission from Elsevier. (c) The organic semiconductor surface functionalized with a biotynilated phospholipid layer that prevents the doping of the organic semiconductor and allows for biomolecule immobilization. (d) *I–V* characteristics of the EGOFET device reported in panel (c).

often required; besides, a reference electrode is needed as for other electrochemical detection systems.

Switching from MOSFETs to OFETs, the ISFET-like configuration sees a gating of the OFET that is produced by directly interfacing the OSC with an electrolyte solution. Two classes of devices are originated: the electrochemical transistors (ECTs) and the electrolyte gated FET (EGOFETs). An example from the production of the Malliaras group is used to briefly describe the ECTs sensing mechanism. An ionic liquid is used as the electrolyte to disperse the glucose oxidase enzyme and a ferrocene redox mediator.[47] The redox-reaction between the glucose and the enzyme (GOx) takes place and cycles back with the help of the Fc/ferricenium ion (Fc^+) couple, which shuttles electrons to the gate electrode. At the same time, cations from the solution enter the OSC and dope or dedope it, affecting in this way the I_{DS} current to a degree that depends on glucose concentration. The transduction mechanism is therefore connected to the doping of the OSC and is usually addressed as electrochemical in nature. Due to the amplification inherent in the transistor, concentrations down to 100 nM of glucose could be detected. Also, for this configuration an electro-active analyte is often required, but they do operate at very low voltages.

Another interesting approach is implemented in the EGOFET sensors where an electrolyte solution directly produces the gating for the OFET (Fig. 10a).

In EGOFETs the dielectric gating is achieved through the formation of a Debye–Helmholtz double layer at the interface between the electrolyte solution and the OSC layer as well as between the electrolyte and gate contact. In fact this double layer holds a very high capacitance (*ca.* 10 μF cm^{-2}) and the device can be operated by ranging V_{GS} and V_{DS} in the sub-volt regime. For bio-sensing purposes a bio-recognition element should be anchored to the OSC, allowing the bio-layer to directly interface to the OSC. Such an architecture indeed holds the problem of directly grafting recognition bio-elements, hydrophilic in nature, to the OSC which is notably highly hydrophobic. In a first example of an EGOFET the grafting of the recognition element involved the whole bulk of the OSC rather than the sole active surface. The sensing showed DNA determination in the 0.1 μM concentration range in pure water while no signal could be detected in saline solution.[40] High ionic concentration in fact ended up doping the OSC, which is not desirable in an EGOFET configuration. A better solution turned out to be the bio-functionalization of either one of the two available Debye–Helmholtz interfaces: gate/electrolyte and electrolyte/OSC. The example reported in Fig. 10b involves the bio-functionalization of the gate electrode with a self-assembled monolayer of a boronic acid that holds a high chemical affinity towards molecules with geminal diol groups such as dopamine.[4] Upon the binding of dopamine a negatively charged boronic ester is formed whose charge is counterbalanced by the dopamine amine group. As this electrical dipole is formed the potential drop at the gate-liquid interface increases, thus causing a current decrease as higher gate voltages are needed to compensate. In this case, involving a dipole rather than a net charge, the sensing effect is on the gate capacitance, rather than on the electrochemical potential. As the small capacitance changes upon formation of the complex can dominate over the in-series large capacitance of the electrolyte, detection of the analyte in the pM regime is feasible, although no assessment of the LOD and the LOQ was provided. A second possibility involves the OSC/electrolyte interface that can be bio-functionalized by anchoring (Fig. 10c) a phospholipid bilayer containing the recognition elements to the OSC according to route (b) of Fig. 8A. In this configuration, a bilayer of zwitterionic PL can be used to both immobilize the biotin recognition element and hinder the electrolyte ion diffusion into the OSC. This is confirmed by the *I–V* characteristics (Fig. 10d) exhibiting very low hysteresis upon forward and backward potential scans along with a low gate leakage current I_G. The sensing mechanism involves an I_{DS} current increase generated this time by the extra gating produced by the streptavidin recognition, as this protein is negatively charged at the operating pH. This time an

overall electrochemical potential increase is seen as proven by the V_T shift towards positive gate potentials. The sensing is proven to be selective as a number of negative control experiments involving a PL layer with no immobilized biotin as well as bare P3HT OSC gave the expected zero response. The LOD and the LOQ, taken from the calibration curve reported in Fig. 3, are down to the nM level and have been measured in the presence of physiologically relevant electrolyte concentrations, namely at an ionic strength comparable to that of blood.[44] Although EGOFET is an interesting sensing structure, the bio-recognition event still takes place either on the gate contact surface or at the bio-layer interface opposite to that with the OSC electronic channel, with the presence of the PL layer further hampering the direct coupling between a bio-recognition event and the electronic channel. Last but not least, reliability problems are connected with the gate contact positioning and the need of a reference electrode has not been definitively ruled out. On the other hand, this configuration allows, for a given interface, the direct control of the potential at the bio-layer/OSC interface.

Another interesting ISFET-like OFET sensing approach, that does not need a reference electrode, is the so called Charge Modulated (CM) OFET. In this extended gate OFET, the gate sensing area and the channel region are physically separated and DNA label-free detection has been reported in the sub nM range.[48] However, in this case the bio-recognition is also limited to charged species and there is, by definition, no direct coupling of the bio-recognition and FET channel. This is however a good experimental tool to measure the sole capacitive effects in a given bio-organic interface.

Indeed, so far the detection with a solid state device has been pushed towards its limits with transistors comprising a single nanostructured semiconducting element. Nanostructured channel materials such as a single silicon nanowire or a carbon nanotube bearing a recognition element on the surface, allow close-coupling between the bio-recognition event and the field-induced transport along with a conveniently low interaction cross-section; both concur to achieve extremely sensitive electronic responses allowing the detection of a single molecule. The bio-recognition element is anchored to the nanostructured semiconductor surface and electrolyte gating is mostly adopted, although back-gating through oxide dielectrics is also used. As far as the biotin–streptavidin assay is concerned the lowest detection was achieved with a biotinylated Si nanowire capable to sense down to 25 pM.[49] The main drawbacks of these achievements, otherwise challenging and fascinating, are the technological issues inherent to a nano-device; reliable fabrication that impacts on the response repeatability, limiting the overall quality of the data set in the systematic investigations needed to shed light on bio-electronic transduction mechanisms. High-cost production and the difficult scalability are also issues. Conversely, OFETs can be fabricated by a low-cost, large-area printing procedure. Recently back-gated OFETs have also been proposed for high performance electronic bio-sensing. Indeed this approach produces a label-free response and there is no need for a reference electrode. At first the bio-recognition element was deposited/grafted on top of the OSC layer. This structure, known as the Bi-Layer (BL)OFET, is reported in Fig. 11.

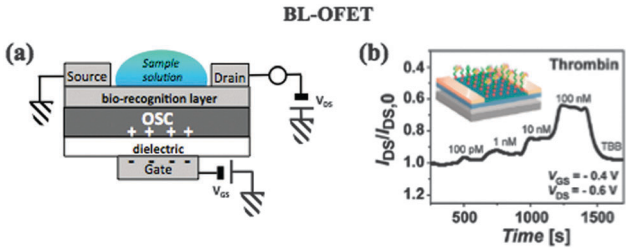

Fig. 11 (a) Bottom gate-top contact OFET biosensor having a bi-layer structure in which the bio-recognition layer is deposited on the organic semiconductor surface. (b) Normalized I_{DS} current changes upon thrombin exposure of an OFET decorated with gold nanoparticle (AuNP) binding sites for thrombin protein DNA binding aptamers. Reprinted from ref. 45, copyright© 2013 American Chemical Society, reproduced with permission from the American Chemical Society.

One of the first papers dealing with this structure involved the deposition of amino acid or glucosidic units on the OSC to endow the OFET with chiral-recognition capability. Indeed, electronic chiral differential detection was achieved for citronellol and carvone enantiomers at the ppm concentration level, pushing the limit of solid-state chiral determination down by three orders of magnitude.[28] Fig. 11b shows the response of a water-stable OFET whose S and D electrodes are protected with a thin layer of SiO_x and the OSC is decorated with an ordered array of AuNPs, as described in Fig. 8B. Thrombin-specific aptamers are attached to the AuNPs *via* Au–S linkages, and the device surface is blocked against nonspecific protein adsorption with bovine serum albumin (BSA). Upon exposure to the target protein, the aptamers bind to thrombin. The current is seen to scale linearly with the logarithm of the concentration as expected in FET-type sensors and negative control was achieved when no capturing molecule was immobilized on the OSC surface. The selective detection of thrombin was successfully achieved down to 100 pM. The ionic strength and pH of the buffer as well as the density of the receptor sites affected the detection profile. Investigation of the effect of the buffer's ionic strength on detection revealed that, while charge screening prohibits charge-based OFET thrombin detection at high (140 mM) ionic strengths, this limitation may be overcome by a suitable reduction in ionic strength. In general, increasing the overall net charge of the protein analyte resulted in increased sensitivity.

The response of bottom gate OFETs bearing sulfate binding protein immobilized on top of the semiconductor has been also proposed. In this case, the immobilization was accomplished on the surface of an extra insulating layer also deposited on the OSC. The insulating layer consists of maleimide functionalized polystyrene (PSMI), capable of anchoring the protein recognition element. The device was exposed just to 1mM Na_2SO_4 solution and measured under dry conditions. An effective charge per protein of $-1.7q$ was estimated form the threshold shift, being quite close to the $-2q$ expected value as each protein should capture one SO_4^{-2}.[50]

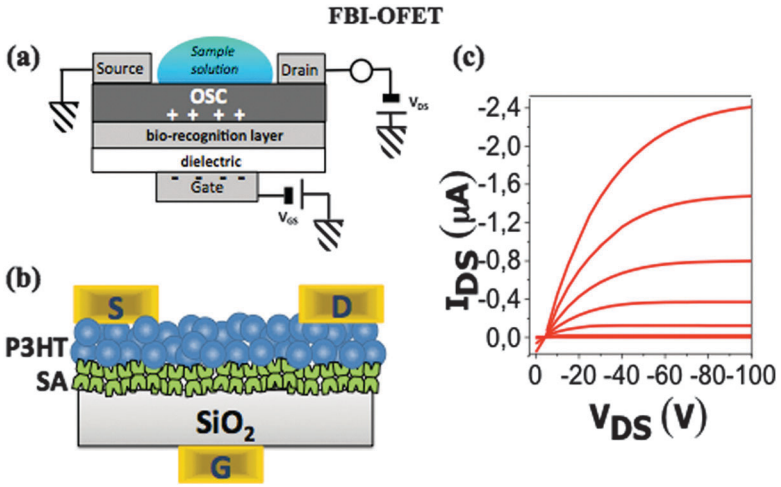

Fig. 12 (a) Bottom gate-top contact OFET biosensor having a FBI structure in which the bio-recognition layer is deposited directly at the dielectric and organic semiconductor interface. (b) FBI-OFET embedding a streptavidin bio-recognition layer along with typical *I–V* characteristic curves in panel (c).

A bottom gate OFET functionalized with PNA as described in route (a) of Fig. 8A successfully lead to DNA detection at the low nM level by covalently immobilising PNA probes on the OSC surface.[51] Repeatability of the sensors was investigated for two concentrations (100 and 200 nM). Similarly to the previous approach, immobilization of BSA has been realized for the *in situ* detection of anti-BSA.[52] Different concentrations were detected ranging from 10 nM to 2 μM.

The BLOFET structure clearly produced some very interesting results, particularly when implemented with the gold nanoparticles arrays that, while interacting with the analyte, involve charge modifications that reflect on the OSC 2D transport. The sensing mechanisms in BLOFETs, that do not involve charged species, are similar to those already discussed for the OFET chemical sensors although in BLOFET the analyte direct impact on the 2D transport layer is mediated by its selective interaction with the external layer bearing the bio-recognition element. Basically, for not-charged species the external layer acts like a filter retaining aliquots of the analyte. The stronger the interaction, the lesser the amount of analyte percolated down to the interface. To achieve a closer contact between the recognition event and the OSC 2D layer in a BLOFET configuration, an OSC as thin as the 2D transport layer can be used. This approach was pursued by physically adsorbing DNA molecules onto the surface of an ultra-thin pentacene films.[53] Measurements of the electrical performance were carried out in the dry state. The device was exposed to DNA solutions exhibiting a sensitivity of 0.2 μM. Such an approach requires a strict control over the interfacial properties to assure good reproducibility, bringing us back to the stability and reproducibility issues already discussed for the nano-structured FET sensors.

Lately, a novel structure was conceived with the aim of creating a direct interface between the OSC and the capturing molecules. This biosensor comprises an OFET device where the bio-layer is deposited underneath the OSC, resulting in the Functional Biological Interlayer (FBI)OFET[54] depicted in Fig. 12a.

Clearly in such a device an intimate contact is created between the region where the bio-recognition takes place and the OCS FET channel. It foresees also an electronic transduction, though difficult to achieve as the FBI-OFET functions on the basis of a counterintuitive approach involving a FET electronic channel set to work on top of a biological deposit. By knowing how critically the FET transport depends on the dielectric/OSC interface quality and seeing how rough a protein deposit can be, a successful FET transport was evaluated as highly unlikely. In fact, the results reported in Fig. 12c furnish compelling evidence that this is not the case. Fig. 12b shows the FBI-OFET fabricated on a standard rigid Si–SiO_2 substrate, (SiO_2 being 300 nm thick) embedding a streptavidin (SA) bio-layer residing underneath a poly-hexylthiophene (P3HT) thin-film (SA spin-coated from water and P3HT from chloroform). In Fig. 12c the *I–V* characteristic curves are measured on a FBI-OFET, showing that FET transport occurs with figures of merit that, though affected by the integration of the recognition element, are still quite good (μ from 4 to 2×10^{-3} cm^2 V s^{-1}, V_T from 5 to 20 V, on/off ratio from 10^3 to 10^2). Applied biases would have been lower than 5 V if a high-*k* thinner dielectric had been used. An improvement of these figures is foreseen by using a higher mobility OSC (tips-pentacene for instance) and/or by using different deposition procedures (Langmuir–Blodgett, L–B, spray-coatings).

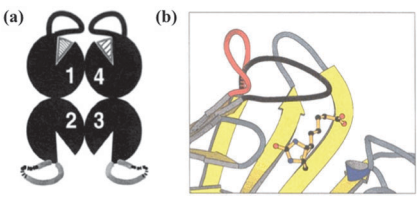

Fig. 13 (a) Schematic structure of streptavidin evidencing the four biotin binding sites and their conformational change after biotin interaction. (b) Detailed structure of a streptavidin recognition site after the biotin binding. Reprinted from ref. 55, copyright© 2000 The Protein Society, reproduced with permission from John Wiley & Sons, Inc.

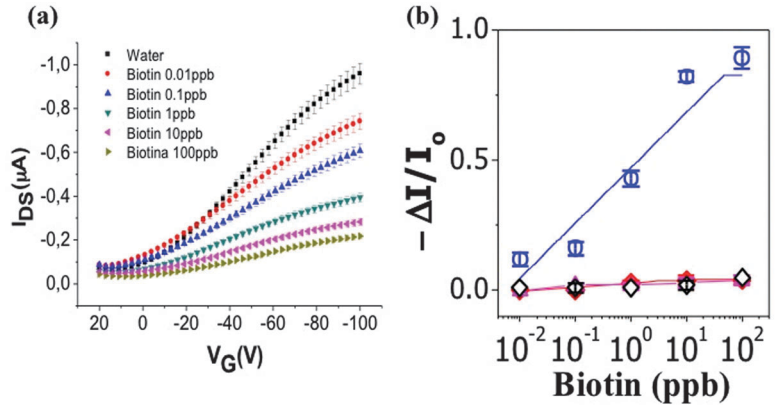

Fig. 14 (a) Typical I_{DS}–V_G curves obtained for a streptavidin FBI-OFET exposed to pure water and biotin solutions at different concentrations. (b) Response of a spin-coated streptavidin FBI-OFET to different biotin concentrations. Each data point is the $\Delta I/I_0$ mean value over three replicates measured on different OFET devices. Error bars are taken as the relative standard deviations. The response to different biotin concentrations for FBI-OFETs embedding other capturing layers used as negative controls is also reported. Triangles: saturated streptavidin–biotin complexes FBI-OFET; squares: P3HT-OFET; diamonds: bovine serum albumin FBI-OFET.

The possibility to have an FET transport on top of a biodeposit opens the door to the direct electronic probing of biorecognition events. It is known that SA has a selective and almost irreversible interaction with biotin, leading to the formation of a very stable complex (with a dissociation constant of fM). In this process, SA undergoes a conformational change which causes the characteristic string loops to close on the incorporated biotin. Biotin binding to SA is depicted in Fig. 13a (biotins are the grey triangles, the SA tetrameric protein is sketched by the four black circles).

Fig. 13b shows a detail of one of the SA lobes, showing how the red loop turns into the black one as the biotin–SA complex is formed.[55] As the FBI-OFET the complex is formed just underneath the OSC, a very sensitive response is expected.

The results of the SA FBI-OFET exposed to biotin solutions of different concentrations (from pM to nM) are reported in Fig. 14a as the relevant *I*–*V* transfer characteristics.

Here a systematic and scalable decrease in the current is observed as the device is exposed to different biotin concentrations, showing that the response appears to be directly connected with the complex formation. The relevant dose curve, reporting the relative current decrease is shown in Fig. 14b. For both panels, error bars, as standard deviations over three replicates on different SA FBI-OFET, show how the current variation is in fact significant even at the lowest concentration (50 pM), this being one of the lowest ever measured, most probably because a direct coupling with the electronic transport is created. It is important to outline that the response is not likely connected to a net charge variation effect. Indeed, it would be extremely interesting to understand if this response is related to the SA loop movement (conformational change) occurring underneath the OSC and possibly affecting the polymer π-conjugation or the local charge. The other data points present in Fig. 14b are relevant to sets of negative control experiments that provide a zero response assessing the selectivity of the streptavidin–biotin interaction in the FBI-OFET assay proposed. Also, error bars are within a few percent while the LOD is 50 pM and the LOQ is 100 pM. The quantification of small molecules is a rather demanding task and, in the case of biotin, nM concentration levels have been detected at most, even with extremely sensitive non electronic determinations such as an electrochemical and a label-needing fluorescent assay, both carried out in solution. The label-free FBI-OFET approach allows the reaching of detection levels that are comparable to those so far achieved by much better performing nanostructured sensors. Also relevant is that the FBI-OFET determination does not need a reference electrode and can be performed also in the case of neutral species. One drawback is the necessity for the analyte to percolate through the OCS layer.

Conclusions

Organic field-effect transistors are presented as label-free, sensitive and selective electronic sensors. This review provides also the most relevant learning points, from the analytical sensor figures of merit to the salient details of the OFET transport. Moreover, details on the bio-functionalization of an OFET device surface are presented. All the major sensor device configurations are introduced, highlighting the most significant achievements along with the limitations. The sensing mechanisms are discussed and important issues such as low-voltage operation as well as the need for a reference electrode or the ability to sense charged or neutral bio-molecules are presented for the different configurations. The assessment of the analytical figures of merit is also highlighted, stressing how the validation of an analytical method is an essential step to prove its capability to provide reliable qualitative or quantitative data. This applies also and more compellingly to a novel technology such as electronic biosensing.

This reviews highlights also how the driving force towards the use of OFETs as biosensors is to combine the electronic output signal and the high sensing performance level with low-cost fabrication to develop disposable electronic sensing systems that would be ideal for POC testing and how electronic biosensing on a disposable strip-test is considered the next paradigm shift in diagnostics.

Acknowledgements

Prof. Annalisa Bonfiglio, Paolo Lugli and Roisin Owens are acknowledged for useful discussions.

Notes and references

1 M. D. Angione, R. Pilolli, S. Cotrone, M. Magliulo, A. Mallardi, G. Palazzo, L. Sabbatini, D. Fine, A. Dodabalapur and N. Cioffi, *Mater. Today*, 2011, **14**, 424–433.
2 L. Kergoat, B. Piro, M. Berggren, G. Horowitz and M.-C. Pham, *Anal. Bioanal. Chem.*, 2011, **402**, 1813–1826.
3 S. Goetz, C. Erlen, H. Grothe, B. Wolf, P. Lugli and G. Scarpa, *Org. Electron.*, 2009, **10**, 573–580.
4 T. Cramer, A. Campana, F. Leonardi, S. Casalini, A. Kyndiah, M. Murgia and F. Biscarini, *J. Mater. Chem. B*, 2013, **1**, 3728.
5 R. M. Owens and G. G. Malliaras, *MRS Bull.*, 2010, **35**, 449–456.
6 P. Lin and F. Yan, *Adv. Mater.*, 2012, **24**, 34–51.
7 A. Dodabalapur, *Mater. Today*, 2006, **9**, 24–30.
8 L. Bisiricò, *et al.*, *Thin Solid Films*, 2011, **520**, 1291–1294.
9 C. Wang, H. Dong, W. Hu, Y. Liu and D. Zhu, *Chem. Rev.*, 2011, **112**, 2208–2267.
10 E. D. Głowacki, M. Irimia-Vladu, M. Kaltenbrunner, J. Gsiorowski, M. S. White, U. Monkowius, G. Romanazzi, G. P. Suranna, P. Mastrorilli, T. Sekitani, S. Bauer, T. Someya, L. Torsi and N. S. Sariciftci, *Adv. Mater.*, 2013, **25**, 1563–1569.
11 N. Ronkainen, H. Halsall and W. Heineman, *Chem. Soc. Rev.*, 2010, **39**, 1747–1763.
12 B. A. McKinley, *Chem. Rev.*, 2008, **108**, 826–844.
13 J. W. Steed, *Chem. Soc. Rev.*, 2009, **38**, 506–519.
14 N. Barsan, K. D. Schierbaum and U. Weimar, *Handbook of Heterogeneous Catalysis*, Wiley-VCH Verlag GmbH & Co. KGaA, 2008, Chemical Sensors Based on Catalytic Reactions.
15 M. Thompson, S. L. R. Ellison and R. Wood, *Pure Appl. Chem.*, 2002, **74**, 835–855.
16 F. Ebisawa, T. Kurokawa and S. Nara, *J. Appl. Phys.*, 1983, **54**, 3255–3259.
17 M. Irimia-Vladu, E. D. G. Irimi, G. Voss, S. Bauer and N. S. Sariciftci, *Mater. Today*, 2012, **15**, 340–346.
18 A. J. Lovinger, D. D. Davis, R. Ruel, L. Torsi, A. Dodabalapur and H. E. Katz, *J. Mater. Res.*, 1995, **10**, 2958–2962.
19 R. A. Street, *Adv. Mater.*, 2009, **21**, 2007–2022.
20 A. Dodabalapur, L. Torsi and H. E. Katz, *Science*, 1995, **268**, 270–271.
21 F. Liscio, *et al.*, *ACS Nano*, 2013, **7**, 1257–1264.
22 G. Horowitz, *J. Mater. Res.*, 2004, **19**, 1946–1962.
23 N. Tessler, Y. Preezant, N. Rappaport and Y. Roichman, *Adv. Mater.*, 2009, **21**, 2741–2761.
24 H. Laurs and G. Heiland, *Thin Solid Films*, 1987, **149**, 129–142.
25 A. Assadi, G. Gustafsson, M. Willander, C. Svensson and O. Inganäs, *Synth. Met.*, 1990, **37**, 123–130.
26 G. Guillaud, M. Al Sadoun, M. Maitrot, J. Simon and M. Bouvet, *Chem. Phys. Lett.*, 1990, **167**, 503–506.
27 L. Torsi, A. Dodabalapur, L. Sabbatini and P. G. Zambonin, *Sens. Actuators, B*, 2000, **67**, 312–316.
28 L. Torsi, G. M. Farinola, F. Marinelli, M. C. Tanese, O. H. Omar, L. Valli, F. Babudri, F. Palmisano, P. G. Zambonin and F. Naso, *Nat. Mater.*, 2008, **7**, 412–417.
29 B. Crone, A. Dodabalapur, A. Gelperin, L. Torsi, H. Katz, A. Lovinger and Z. Bao, *Appl. Phys. Lett.*, 2001, **78**, 2229–2231.
30 L. Torsi, A. Lovinger, B. Crone, T. Someya, A. Dodabalapur, H. Katz and A. Gelperin, *J. Phys. Chem. B*, 2002, **106**, 12563–12568.
31 R. D. Yang, J. Park, C. N. Colesniuc, I. K. Schuller, W. C. Trogler and A. C. Kummel, *Appl. Phys. Lett.*, 2007, **103**, 034515.
32 D. Duarte and A. Dodabalapour, *J. Appl. Phys.*, 2012, **111**, 044509.
33 L. Torsi, M. Tanese, N. Cioffi, M. Gallazzi, L. Sabbatini, P. Zambonin, G. Raos, S. Meille and M. Giangregorio, *J. Phys. Chem. B*, 2003, **107**, 7589–7594.
34 M. Erouel, K. Diallo, J. Tardy, P. Blanchard, J. Roncali, P. Frere and N. Jaffrezic, *Mater. Sci. Eng., C*, 2008, **28**, 965–970.
35 S. Tiwari, A. K. Singh, L. Joshi, P. Chakrabarti, W. Takashima, K. Kaneto and R. Prakash, *Sens. Actuators, B*, 2012, **171–172**, 962–968.
36 A.-M. Andringa, M.-J. Spijkman, E. C. Smits, S. G. Mathijssen, P. A. v. Hal, S. Setayesh, N. P. Willard, O. V. Borshchev, S. A. Ponomarenko, P. W. Blom and D. M. de Leeuw, *Org. Electron.*, 2010, **11**, 895–898.
37 F. Marinelli, A. Dell'Aquila, L. Torsi, J. Tey, G. Suranna, P. Mastrorilli, G. Romanazzi, C. Nobile, S. Mhaisalkar and N. Cioffi, *Sens. Actuators, B*, 2009, **140**, 445–450.
38 J. E. Royer, E. D. Kappe, C. Zhang, D. T. Martin, W. C. Trogler and A. C. Kummel, *J. Phys. Chem. C*, 2012, **116**, 24566–24572.
39 N. J. Tremblay, B. J. Jung, P. Breysse and H. E. Katz, *Adv. Funct. Mater.*, 2011, **21**, 4314–4319.
40 L. Kergoat, B. t. Piro, M. Berggren, M.-C. Pham, A. Yassar and G. Horowitz, *Org. Electron.*, 2012, **13**, 1–6.
41 P. Bergveld, *IEEE Trans. Biomed. Eng.*, 1972, **18**, 342–451.
42 P. Bergveld, *Sens. Actuators, B*, 2003, **88**, 1–20.
43 H. U. Khan, M. E. Roberts, O. Johnson, R. Förch, W. Knoll and Z. Bao, *Adv. Mater.*, 2010, **22**, 4452–4456.
44 M. Magliulo, A. Mallardi, M. Yusuf Mulla, S. Cotrone, B. R. Pistillo, P. Favia, I. Vikholm-Lundin, G. Palazzo and L. Torsi, *Adv. Mater.*, 2013, **25**, 2090–2094.
45 M. L. Hammock, *et al.*, *ACS Nano*, 2013, **7**, 3970–3980.
46 D. T. V. Anh, W. Olthuis and P. Bergveld, *Sens. Actuators, B*, 2003, **91**, 1–4.
47 S. Y. Yang, F. Cicoira, R. Byrne, F. Benito-Lopez, D. Diamond, R. M. Owens and G. G. Malliaras, *Chem. Commun.*, 2010, **46**, 7972–7974.
48 S. Lai, M. Demelas, G. Casula, P. Cosseddu, M. Barbaro and A. Bonfiglio, *Adv. Mater.*, 2013, **25**, 103–107.
49 Y. Cui, Q. Wei, H. Park and C. M. Lieber, *Science*, 2001, **293**, 1289–1292.

50 F. Maddalena, M. J. Kuiper, B. Poolman, F. Brouwer, J. C. Hummelen, D. M. de Leeuw, B. De Boer and P. W. Blom, *J. Appl. Phys.*, 2010, **108**, 124501–124504.
51 H. U. Khan, M. E. Roberts, O. Johnson, R. Forch, W. Knoll and Z. Bao, *Adv. Mater.*, 2010, **22**, 4452–4456.
52 H. U. Khan, J. Jang, J.-J. Kim and W. Knoll, *J. Am. Chem. Soc.*, 2011, **133**, 2170–2176.
53 P. Stoliar, E. Bystrenova, S. Quiroga, P. Annibale, M. Facchini, M. Spijkman, S. Setayesh, D. De Leeuw and F. Biscarini, *Biosens. Bioelectron.*, 2009, **24**, 2935–2938.
54 D. Angione, *et al.*, *Proc. Natl. Acad. Sci. U. S. A.*, 2012, **109**, 6429–6434.
55 S. Freitag, I. Le Trong, L. Klumb, P. S. Stayton and R. E. Stenkamp, *Protein Sci.*, 1997, **6**, 1157–1166.

